



Contents lists available at CEPM

Computational Engineering and Physical Modeling

Journal homepage: www.jcepm.com



Debonding and Fracture Behavior of Concrete Specimens Retrofitted by FRP Composite

H. Abbaszadeh^{1*} , A. Ahani¹, M.R. Emami Azadi²

1. M.Sc. Student, Faculty of Civil Engineering, Istanbul Technical University, Istanbul, Turkey

2. Assistant Professor, Faculty of Civil Engineering, Azarbaijan Shahid Madani University, Tabriz, Iran

Corresponding author: abbaszadeh17@itu.edu.tr

 <https://doi.org/10.22115/CEPM.2018.125309.1015>

ARTICLE INFO

Article history:

Received: 17 March 2018

Revised: 15 June 2018

Accepted: 16 June 2018

Keywords:

Fracture behavior of concrete;

Fracture parameters;

FRP composites;

Debonding.

ABSTRACT

The effects of FRP retrofitted concrete specimens with couple of notches on the fracture behavior have been investigated during an experimental and analytical test program in this study. This paper represents the fracture characteristics and parameters for three point bending tests on two distinguish retrofitted and plain condition for both intact and notched (couple notches) specimens. The experimental test results find out in the laboratory tests indicated that for intact concrete specimens, there would be approximately 285% increase in ultimate flexural strength tests. The experimental results also represents that for the tested couple notched concrete specimens, there might be approximately 318% increase in ultimate flexural strength. Based on the analytical study, it is found that the near failure behavior of the notched specimens have been significantly improved using FRP retrofit of such specimens. The system's global energy balance and failure load prediction of FRP debonding are the couple of consideration by a developed fracture mechanics based model which made by energy dissipation major mechanisms characterizing while debonding. Model verification is provided using previous researches experimental data from literature. In addition, fracture mechanics parameters were found out for three point bending test in this paper for better understanding on fracture behavior and fracture properties of intended specimens.

How to cite this article: Abbaszadeh H, Ahani A, Emami Azadi MR. Debonding and Fracture Behavior of Concrete Specimens Retrofitted by FRP Composite. *Comput Eng Phys Model* 2018;1:27–40. <https://doi.org/10.22115/cepm.2018.125309.1015>

2588-6959/ © 2018 The Authors. Published by Pouyan Press.

This is an open access article under the CC BY license (<http://creativecommons.org/licenses/by/4.0/>).



1. Introduction

In recent years, implementation of fiber reinforced polymers (FRP) in order to external retrofitting of reinforced and plain concrete structures become more considerable case, especially in the form of sheets and laminates. This depends on the competitive mechanical properties of the composite material, and the in-situ installation method which is commonly straight forward. However, implementing this method needs that local failure modes to be considered both for that end. In the recent years, the scientific community has completed some significant experimental and analytical works to have proper prediction and comprehension of the bond behavior between concrete (specifically surface) and FRP sheets [1].

An international effort is processing to progress well organize guidelines and codes to manage the standards for material selection, design, installation, inspection, maintenance, and retrofit of FRP applications. Approved conventional design approaches with developments to consideration of the presentment and characteristics of the FRP material is the fundamental approach to designing structural retrofitting projects by implementation of externally bonded FRP composites. However, non-conventional designing approaches need specific attentions and considerations for suitable coverage in the design development. The common debonding problem is one of these designing issues, which occurs for externally retrofitted FRP elements, this problem state in the research section of designing as the knowledge about this method is in elementary levels [2–4]. Design methods and procedures, which suitably consider debonding problems are required to guaranty reliability and the safety of bending elements retrofitted by the intended FRP composites. This research represents firstly an experimental and secondly an analytical study to have better understanding about debonding failures in FRP retrofitted specimens, fracture characteristics to have better estimation of failures like this for considering them in designing the different systems.

Failure of FRP retrofitted specimens such as beams like specimens in this study may occurs through several mechanisms depending on retrofitting parameters and specimen itself. In the ACI 440 Committee code on Fiber Reinforced Polymer Reinforcement [5,6], modes of failure are considered as: (a) crush in concrete before reinforcement yields, (b) concrete crushing, (c) cover delamination, (d) FRP rupture associated with steel yielding, (e) FRP debonding.

Nomenclature

a	notch length	G_C	critical energy of fracture
S	support distances from each other	G_{IC}	first mode critical fracture energy
L	length of the specimen (beam)	G_F	fracture energy
B	width of specimen	f_t	tensile strength
W	height of specimen	$\sigma(w)$	shape of softening curve
K	fracture toughness	g	maximum aggregate size
K_{IC}	first mode critical fracture toughness	w	crack opening
M_{max}	maximum moment applied to section	f'_c	compressive strength of concrete
σ	stress that was provide fracture failure		
G	energy release due to a unit extension of a crack of unit width		

Oehlers [7] characterized the debonding failure modes based on the type of cracks which causes debonding. Furthermore, shear failure take place if at the increasing point of flexural capacity the shear capacity cannot accommodate it. An investigation needed on failure modes to guaranty that the design element works correctly as it considered. In addition, initiation and propagation of debonding process lead to a dramatic reduction in element capacity which is occurs associated with a debonding failure [1].

Modeling and characterization of debonding in structural elements retrofitted by using externally bonded reinforcements method has become a famous area of study as there are several critical significance of bonded joints debonding failures. In recent decades, multitude research works was performed, with considering the importance of FRP retrofitted flexural members and effects of FRP composites on elements, and some developed process has been obtained comprehension the reasons and debonding failures mechanisms on several researches [8,9].

The interfacial stress distribution calculation for FRP retrofitted elements using strength approach require estimation of debonding failures based on properties of elastic material. In addition, the belief that debonding is a phenomena which occurs following propagate of crack propagation by stress of local forces, increase the interest toward implementing some research works toward obtain an approach using fracture mechanics methods to solve the problem by providing models which uses both fracture and elastic material properties that is used for prediction also [8]. Some of recent researches have studied on opening mode, mixed mode and shear mode fracture processes within the development of debonding process.

Gunes [10], and Achintha and Burgoyne [11] could estimate the debonding failure loads using the balance of global energy in a retrofitted beam, considering an approach of fracture mechanics with basic differences in fracture debonding and energy components characterization. There are also several problems which needs an explanation in the clarification of the bond between retrofitted material and concrete. Different researchers have provided test models for pure shear to develop fundamental relation for the concrete-to-FRP interface forces. [12]. During this work it is supposed that the loading on FRP composites: (1) was applied aligned to the concrete specimen axis; and (2) was completely parallel with the symmetry axis of retrofitted concrete specimens. Particularly, a peel test configuration with mixed-mode debonding was implemented by Lorenzis and Zavarise [13].

The stress concentration taking place at the limit portion of the FRP can lead to immature collapse of the retrofitted concrete element. The local failure of mentioned type usually take place through a narrow layer of concrete connected to the epoxy-fiber layers, after that remains safe. The significance of intended event is literally related to the energy dissipation value per cracked surface area unit, that includes a consideration of both mode-I and mode-II fracture, that was determined by fracture in mixed mode. Many research and detailed studies have been performed to recognize this behavior. However, these material parameters explanation was not provided clearly and conflicting outcomes are obtained since recent years. For example, Bazant and Pfeiffer [14] and Ozbolt, Reinhardt [15] proposed mode-II fracture energy values circa 25 times greater than the fracture energy; however, Täljsten [16] implemented both shear and compression stresses experimental tests and suggested a ratio of around 10.

Armanios [17] used cracked-lap-shear configuration in order to study the inter-laminar behavior (fracture) of graphite/epoxy composites. In order to predict fracture behavior single model for damage growth was presented. Ivens et al. [18] obtained that the primary inter-laminar fracture toughness increased associated with the treatment level of fiber surface, these outcomes was found during the study on carbon fiber reinforced polymer composites of mode I, mode II and mixed mode fracture [19]. Moreover, in order to clarify the procedure which causes the interface fracture toughness to effect the primary fracture toughness, a model (micromechanical) was made. Ni et al. [20] did research on the inter-laminar fracture mechanism of some common carbon fiber reinforced polymer. Based on their study, the inter-laminar fracture toughness was dramatically affected by the bridging. Based on the adhesive force model the inter-laminar fracture toughness enhancement was predicted, also. Rikards et al. [21] studied the glass fiber reinforced polymer composites in order to find out mode I, mode II and mixed mode inter-laminar fracture properties through the tensile tests (compact type).

Furthermore, the thick-section pultruded FRP composites was studied in order to model the fracture failure which was made by crack-like flaws the fracture characteristics. Haj-Ali et al. [22] developed many experimental and also analytical researches on the mode I and mode II fracture characteristics of pultruded glass fiber reinforced polymer composites. A nonlinear fracture analysis was provided and a calibrated cohesive modeling made to estimate the crack growth for different crack sizes. Based on previous studies, building the model of cohesive zone was the probable affected theory which leads to analysis the fracture characteristic of pultruded FRP [23].

An important issue through the failure behavior of FRP retrofitted specimens is the interaction between debonding and shear failure mechanism that could give abnormal relation and final happening. Debonding failure and debonding + shear failure incorrect differentiation and report was responsible for this occurrence. However, the ductility behavior is the basic significant difference between debonding and shear failures [1,10].

In flexural retrofitting of concrete specimens (beams) the reasons which reduce the efficiency of the externally bonded FRP sheets is immature FRP debonding. Creation and propagate of major crack in the FRP-concrete interface place causes debonding initiation. Thus, in order to obtain the failure load in many previous studies finite element methods based on fracture mechanics rules was used generally. Hutchinson and Suo [24] initial theories were the fundamental for these analyses usually, that were predesignated for the analysis and evaluate the thin-layered elastic materials interface debonding. However, in comparison with some materials such as glass, concrete fracture process zone is considered large, usually with the width of very greater than aggregates and around 300 mm length [25]. Thus, the concrete-FRP interface model could not be developed using the linear elastic fracture mechanics (LEFM) approaches [26].

A high stress can cause a crack to begin forming near the interface (i.e. hot spot); however, the intended crack will propagate at the time which, more energy is therewith released than it requires to creat the new fracture surfaces. Hence, a close way could not be find out based on a precise and well provided stress analysis from procedures as this problem is a fracture mechanics. In previous provided nonlinear fracture mechanics models in literature, the results of

shear-lap tests were performed to find out the fracture characteristics which control FRP debonding in FRP-concrete interaction. However, due to existence of great difference between the fracture mode which happens in shear-lap experiments and that in retrofitted beams, intended tests was not obtained precise fracture characteristics which could be applied in the related analysis. Furthermore, the critical interface crack was created due to enduring a great tension force by FRP. Thus, tensile fracture created by a great tension at the crack tip. Oehlers et al. [27] represented a model, which occur at the major flexural crack based on the rigid-body rotations which causes debonding.

The assumption in model was unavoidable flaws in the interface, and debonding will take place when there is an energy which runs a propagation of an existing interface crack outrage the energy which is required to create the new surfaces based on model predictions. In order to specify debonding in the model, two main controlling parameters are compared; the rate of energy release (i.e. the energy release due to a unit extension of a crack of unit width— G) and the interface fracture energy (the energy needed to create a new fracture surfaces required to combine a unit extension of a crack of unit width— G_{F_int}). Producers have now provided enough tough adhesives that, failures occurs in the concrete just above the interface generally (see Fig. 1). So, it is feasible to assume that G_{F_int} is equal to the concrete fracture energy (G_C). The critical crack – i.e. the smallest available crack which under the existing conditions could propagate rapidly – could be obtained when $G = G_C$. The model could be derived in two way for an intended beam; (i) crack length (which causes failure of beam at the design load), and (ii) failure load (a known length of a beam with an existing crack). In addition, test data which is reported by previous researches matched well with predictions of this model and adopted in the analysis based on this concept [28].

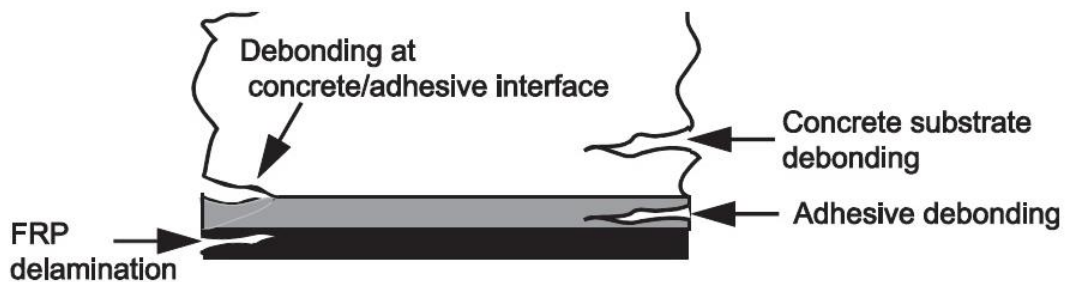


Fig. 1. Different interface crack initiation possible phases [26].

In this research, fracture properties and debonding failure of (i) notched un-retrofitted concrete, and (ii) retrofitted notched concrete specimens (beam) was provided after performing the test and final results was compared by previous works [1,26]. Furthermore, the test that was made in this work is a three-point bending test with couple of notches instead of one notch, and the outcomes for fracture parameters was shown for finding out the differences between previous researches that was generally made by four-point test with single notch.

2. Experimental work

2.1. Test specimens

A total of 12 unreinforced concrete specimens were tested for Flexural strength. The FRP laminates were applied directly to the substrate surfaces of the specimens.

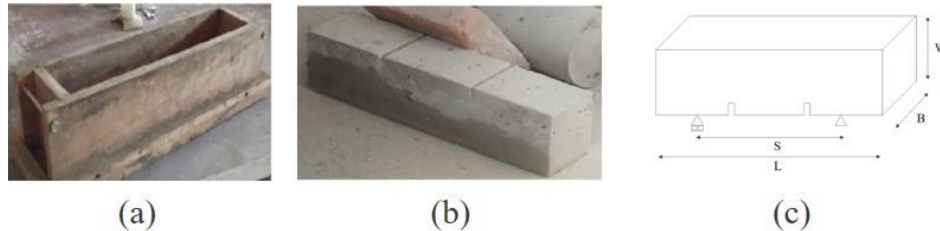


Fig. 2. Specimen a) mold, b) notched form, and c) dimensions.

Fig. 2 shows the shape of specimen with dimensions ($L=38$ (cm), $S=24$ (cm), $B=8$ (cm), and $W=11$ (cm)) and the mold which was used for specimens.

2.2. Testing procedure

After 28 days which is require for curing of the concrete specimens, they were ready for flexural or bending test. Fig.2c shows the dimension of notched part ($a=10$ (mm)) and machine grooved (notched) specimen. Half of specimens were grooved by using a hand cutting machine. Then, the test specimens were retrofitted by using FRP composite sheets as shown in Fig. 3a.

After cleaning the surfaces of specimens and making them ready for application of theFRP composites, 3-4 millimeter Epoxy Dur 300 was applied to the surfaces then FRP sheets were attached to the bottom surface of the specimens. Afterwards, 2-3 millimeter Epoxy Dur 300 glue was applied for final covering of the CFRP sheets. The concrete specimens after retrofitting could be observed in Fig.3a which is ready for flexural testing.

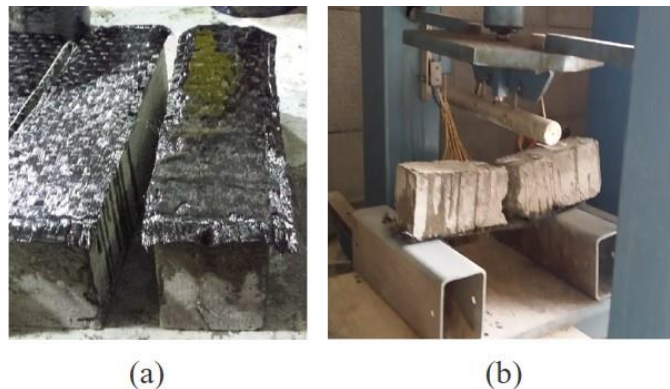


Fig. 3. a) Retrofitted specimens, and b) Test (after failure).

After 4 days that was required for curing of FRP composites, the testing procedure had started. The flexural test procedure was according to ASTM C29 standard [28] and testing was

performed at 23 in laboratory. A concrete specimen at the end of flexural testing is shown in fig. 3b.

2.3. Experimental results

The Flexural strength testing results were obtained for different conditions (intact specimens, grooved or notched specimens, retrofitted intact specimens, and retrofitted notched or damaged specimens).

Table 1.

Flexural strength of the tested specimens (MPa).

Specimen condition	Specimen 1	Specimen 2	Specimen 3	Average
Intact specimen	4.272	4.45	4.38	4.367
Retrofitted intact specimen	14.59	18.15	16.00	16.24
Notched specimen	3.84	4.05	3.91	3.93
Retrofitted notched specimen	18.51	15.66	15.30	16.49

Table 1 shows, 285% increase in average ultimate flexural strength of the tested specimens due to retrofitting by FRP sheets. In specimens testing, the concrete section was initially cracked but the FRP laminates attached to the concrete specimen had increased the flexural resistance of the retrofitted section until the ultimate stage of the tests (see for e.g. Fig. 5(c)).

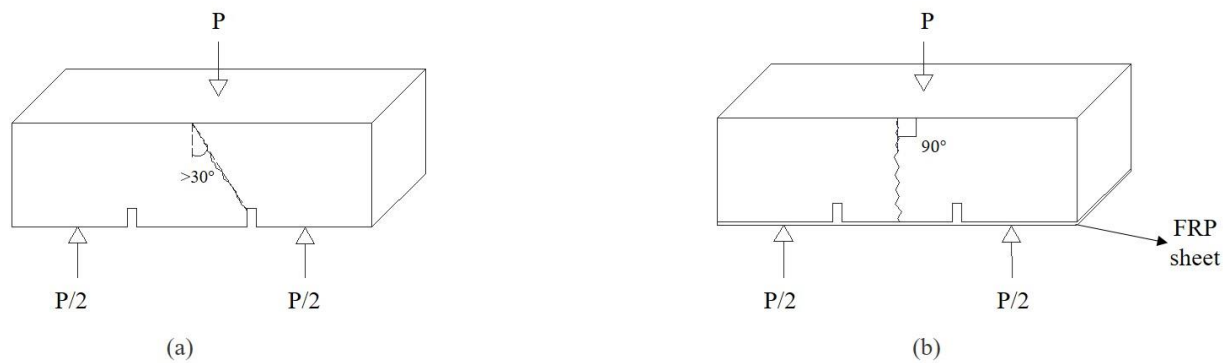


Fig. 4. Fracture (crack line) for a) un-retrofitted specimen b) Retrofitted specimen.

A partial debonding of FRP composite was observed at near ultimate failure of the tested specimens. The partial debonding of CFRP sheet has taken place in a layer of concrete as shown in Fig. 5c. The test results as given in Table 7 might indicate that there is no very significant difference in flexural strength between the retrofitted intact concrete specimens and the retrofitted notched concrete specimens.

The most important point in Flexural testing was the difference in slopes of cracks or lines of failure for tested intact, notched and retrofitted intact and retrofitted notched specimens. For intact specimens, the main cracks initiated during testing had angles of 20° - 30° with the vertical axis (Fig. 4(a)); however, the major cracks occurred in the retrofitted (confined) specimens during testing were almost vertical (Fig. 4(b)). In notched specimens testing, the main cracking has occurred with angles of slightly greater than 30° with the vertical axis; however, in retrofitted notched specimens testing, FRP jacketing affected the failure mechanism and the slope of the major cracks were almost vertical.

In testing of specimens, most FRP sheets did not fully rupture under loading (Fig. 5). This shows that, the bonding created between the concrete and FRP sheets had great influence on its performance under flexural loading. Hence, it is found that the complete and effective bonding between concrete and the FRP sheets would be crucial in increasing the ultimate strength of the retrofitted both intact and notched specimens.

3. FRP debonding

The beginning of debonding is relative with the zones and plate end, where interface flaws due to spreading of flexural cracks, intermediate-crack-induced (IC) and plate-end (PE) debonding are two modes which referred to, respectively [11]. High moment zone is the area which IC debonding begins and then propagates through a low moment zone whereas, FRP end is the area which PE debonding begins at the proximity of that and propagates through the middle of the beam (Fig. 5(a)). Debonding in concrete elements commonly occurs in PE debonding; however, in some special cases a thin concrete layer detaches in IC debonding [10].

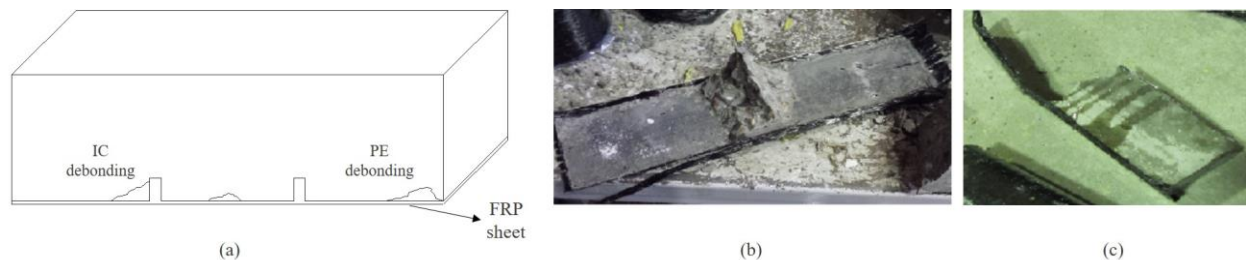


Fig. 5. a) Modes of debonding b) IC debonding, and c) PE debonding.

3.1. Concentration of interfacial stress

A crack in a material could initiate and propagate in three ways; (i) Mode I (opening), (ii) Mode II (shearing which occurs between the faces of a crack), and (iii) Mixed mode (a combination of both mode I and II). Though cracks in isotropic, brittle, homogeneous solids grow by protected pure Mode I position at the tip of crack, debonding at an interface which made by stress field may be very complicated in most cases. Different types of stress concentrations models may develop in order to various fracture toughness values of the two materials such as concrete and FRP and due to of geometric constraints in the interface zone, also [24].

Debonding occurs due to a complicated field of stress, which propagates in the proximity of a critical interface crack. Due to determining the loads at which debonding takes place, an in depth

knowledge about concrete fracture energy related to the mixed-mode loading is required, it will be corrected which the Mode I has an influence on dominate the development of debonding, although [26].

4. Fracture characteristics

For determining fracture behavior finding out fracture parameters is the most important issue that should be considered in fracture studies. In this part some parameters for Linear Elastic Fracture Mechanics (LEFM) and Non-linear Fracture Mechanics (NLFM) was determined for concrete and comparison of intended results by previous research by Arduini et al. [29], Quantrill et al. [30], Jones et al. [31], Ross et al. [29], Garden et al. [32], Fanning and Kelly [33], and Nguyen et al. [34] using the (1) Bilinear mode by Gustafsson and Hillerborg [35], and Guinea et al.[36] , (2) Polynomial mode by Reinhardt [37], and (3) Empirical mode by Bazant and Becq-Giraudon [38] was represented.

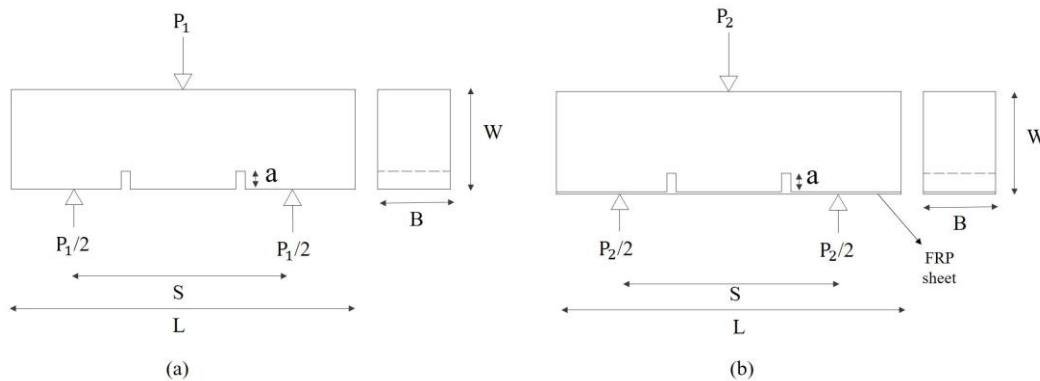


Fig. 6. a) Un-retrofitted specimen, b) Retrofitted specimen

Fig. 6a-6b demonstrates the dimensions and applied load locations such that $P_1 = 46333$ (N), $P_2 = 11066$ (N), $a = 0.002$ (m), $W = 0.11$ (m), $B = 0.08$ (m), $S = 0.240$ (m), $L = 0.380$ (m).

4.1. Linear elastic fracture mechanics for concrete

From the physical point of view, it is clearly obtained that as crack initiation may be relative with stress, the actual creation of cracks needs a specific energy that called fracture energy which represent the surface energy of a solid (BAZANT. [38]). The toughness of a material is controlled by the energy absorbed from the crack propagation [39]. Fracture toughness of a) un-retrofitted specimen $(K)_a$, and b) retrofitted specimen $(K)_b$ and, Critical Fracture toughness in first mode (K_{Ic}) are determined by (3), and (5) respectively,

$$\alpha = \frac{a}{W} = 0.018 \quad (1)$$

$$Y(\alpha) = \frac{[1.99 - \alpha(1 - \alpha)(2.15 - 3.93\alpha + 2.7\alpha^2)]}{(1 + 2\alpha)(1 - \alpha)^{3/2}} = 1.937 \quad (2)$$

$$K = Y(\alpha)\sigma\sqrt{\pi a} \rightarrow \begin{cases} (K)_a = 1.81 \text{ MPa}\sqrt{\text{m}} \\ (K)_b = 7.59 \text{ MPa}\sqrt{\text{m}} \end{cases} \quad (3)$$

$$K_{Ic} = \frac{6Y(\alpha)M_{max}\sqrt{a}}{BW^2} = 1.471 \text{ MPa}\sqrt{\text{m}} \quad (4)$$

As it is shown in (3) and (4), K_{Ic} is not equal to K thus, condition of mode I crack propagation (critical state) cannot be represent in terms of the stress intensity factor. Fracture energy was determined by (6) and as concrete is a quasi-brittle material so, the values of G_F and G_C is equal to each other so,

$$\alpha_F = \frac{1}{4}g + 2 = 6.75 \quad (5)$$

$$G_C = G_F = \alpha_F(f'_c)^{0.7} = 81.311 \text{ (N/m)} \quad (6)$$

4.2. Nonlinear fracture mechanics for concrete

The reason that concrete behavior altered from LEFM to NLFM is the propagation of a relatively large fracture process zone that micro cracking occurs and a developed softening damage take place (see fig. 7-a). This micro cracking effects are: (a) the flux of energy reduction, which could be flows into the crack tip, and (b) in associated with increasing the combined cracking surface area, and then increase the fracture process zone energy absorption capability.

Thus, in the fracture model a relation explaining the softening damage requires to be mentioned. There are couple of ways to represent the intended relation: (i) stress-displacement relation form for the line crack's front zone, or (ii) a stress-strain relation for the strain softening (micro cracking) zone against the major crack. (Bazanat, [40]). In a brittle material such as glass, the energy absorbed from the crack propagation is just that of rupturing the chemical bonds along the crack plane. However, bond rupture has less effect in resisting crack growth in tougher materials, and greater amount of the fracture energy being associated with plastic flow near the crack tip [41]. Fracture Energy G_F could be find out either by area under fig. 7-b curve (8) or by using (7).

$$G_F = \frac{w}{(W-a)B} = \frac{w_0 + 2P_w\delta_0}{(W-a)B} \quad (7)$$

$$G_F = \int_0^{w_c} \sigma(w)dw \quad (8)$$

$$G_{Ic} \approx G_f \approx 0.4G_F \quad (9)$$

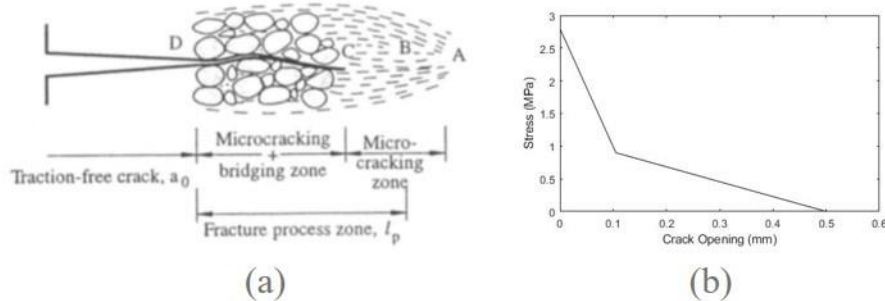


Fig. 7. a) Crack propagation zone, b) Tensile strength-crack opening ($f_t=1.7$ MPa).

The global-energy-balance FRP debonding analysis was applied to many sets of specimens and test results was reported in the literature by previous studies [26]. The G_{Ic} is a significant parameter that was not researched and studied adequately therefore, this research work which was provided by the concrete that its strength (f_c') were in range 40-50 (MPa) and with crushed 20 (mm) aggregate size (Emami and Abbaszadeh, [41]); moreover the magnitude of crack opening (w) assumed to be 500(μm).

Table 2.

The G_{Ic} value based on models for previous and this work [26].

Aggregate Size and Type	Previous works	Models			
		Bilinear		Polynomial	Empirical
		Gustafsson and Hillerborg (1985)	Guinea et al. (1994)	Reinhardt (1985)	Bazant and Becq-Giraudon (2001)
10 mm Rounded	Arduinietal.(1997)	N/A	N/A	N/A	0.068
	Quantrilletal.(1996)	N/A	N/A	N/A	0.073
10 mm Crushed	Jonesetal.(1988)	0.12	0.10	0.08–0.11	0.10
	Rossetal.(1999)	0.13	0.11	0.09–0.13	0.11
	Gardenetal.(Beam 3U,1.0) (1998)	0.12	0.10	0.08–0.11	0.10
20 mm Crushed	FanningandKelly (2001)	0.18	0.17	0.12–0.21	0.13
	Nguyenetal. (2001)	0.15	0.14	0.10–0.18	0.12
	Gardenetal.(Beam 1U,4.5) (1998)	0.15	0.14	0.10–0.18	0.12
	This Work	0.14	0.13	N/A	N/A

5. Conclusion

FRP sheets become more popular for retrofitting the structures and specifically concrete elements; however, the debonding issue and fracture behavior of the intended retrofitted elements are couple of significant problems which effect the performance of this method. Experimental tests indicate that the FRP sheets altered the fracture behavior of specimens; moreover, the crack starts to propagate by opening in the tip. Although the interface of a

retrofitted specimen is primarily enduring shear forces, it commonly fails under tensional forces. So, FRP debonding process behave in Mode I fracture in concrete.

Even though it is obvious that there is need for large specimen to evaluate the fracture behavior of concrete, it is acceptable to suppose that the debonding analysis should be performed with the fracture energy which is obtained using small specimens as it is retrofitted by FRP composite.

Fracture parameter such as K , K_{Ic} , G , G_F , G_{Ic} which were determined for test specimens showed that there is a few differences for single notched and coupled notched specimen in three-point bending but it is not much significant as crack growth forwarded through one of notches.

A model for fracture was provided in this experimental and analytical research, to predict failures of FRP debonding and fracture behavior of plain and retrofitted specimens. The model was applied to several sets of independently reported experimental data from previous researches represented that the results are reliable almost for G_{Ic} .

References

- [1] Gunes O, Buyukozturk O, Karaca E. A fracture-based model for FRP debonding in strengthened beams. *Eng Fract Mech* 2009;76:1897–909. doi:10.1016/j.engfracmech.2009.04.011.
- [2] Kaiser HP. Strengthening of reinforced concrete with epoxy-bonded carbon-fiber plastics. Dr Thesis, Diss ETH 1989.
- [3] Meier U. Strengthening of structures using carbon fibre/epoxy composites. *Constr Build Mater* 1995;9:341–51. doi:10.1016/0950-0618(95)00071-2.
- [4] Buyukozturk O, Hearing B. Failure Behavior of Precracked Concrete Beams Retrofitted with FRP. *J Compos Constr* 1998;2:138–44. doi:10.1061/(ASCE)1090-0268(1998)2:3(138).
- [5] ACI 440, Guide for the design and construction of externally bonded FRP systems for strengthening concrete structures, ACI 440.2R-02, American Concrete Institute, 2002 n.d.
- [6] ACI 440, Report on fiber-reinforced polymer (FRP) reinforcement for concrete structures, ACI 440.R-07, American Concrete Institute, 2007 n.d.
- [7] Oehlers DJ. FRP Plates Adhesively Bonded to Reinforced Concrete Beams: Generic Debonding Mechanisms. *Adv Struct Eng* 2006;9:737–50. doi:10.1260/136943306779369482.
- [8] Buyukozturk O, Gunes O, Karaca E. Progress on understanding debonding problems in reinforced concrete and steel members strengthened using FRP composites. *Constr Build Mater* 2004;18:9–19. doi:10.1016/S0950-0618(03)00094-1.
- [9] Teng JG, Chen J-F, Smith ST, Lam L. FRP: strengthened RC structures. 2002.
- [10] Gunes O. A fracture based approach to understanding debonding in FRP bonded structural members. 2004.
- [11] Achintha PMM, Burgoyne CJ. Fracture Mechanics of Plate Debonding. *J Compos Constr* 2008;12:396–404. doi:10.1061/(ASCE)1090-0268(2008)12:4(396).

- [12] Neto P, Alfaiate J, Dias-da-Costa D, Vinagre J. Mixed-mode fracture and load misalignment on the assessment of FRP-concrete bond connections. *Compos Struct* 2016;135:49–60. doi:10.1016/j.compstruct.2015.08.139.
- [13] De Lorenzis L, Zavarise G. Modeling of mixed-mode debonding in the peel test applied to superficial reinforcements. *Int J Solids Struct* 2008;45:5419–36. doi:10.1016/j.ijsolstr.2008.05.024.
- [14] Bažant ZP, Pfeiffer PA. Shear fracture tests of concrete. *Mater Struct* 1986;19:111.
- [15] Ozbolt J, Reinhardt HW, Xu S. Numerical studies on the double-edge notched mode II geometry. *Proc Fram* 1998;2:773–82.
- [16] Täljsten B. Plate bonding: Strengthening of existing concrete structures with epoxy bonded plates of steel or fibre reinforced plastics 1994.
- [17] Armanios EA. Interlaminar Fracture in Graphite/Epoxy Composites. *Key Eng Mater* 1991;37:85–102. doi:10.4028/www.scientific.net/KEM.37.85.
- [18] J.Ivens, M.Wevers, I.Verpoest, P.Albertsen, M.Peters. Interlaminar fracture toughness of CFRP influenced by fibre surface treatment: Part 2: modelling of the interface effect. *Compos Sci Technol* 1995;54:147–159.
- [19] Albertsen J, Ivens P, Peters M, Wevers I, Verpoest. Interlaminar fracture toughness of CFRP influenced by fibre surface treatment: Part 1: Experimental results. *Compos Sci Technol* 1995;54:33–45.
- [20] Iwamoto M, Ni Q-Q, Fujiwara T, Kurashiki K. Intralaminar fracture mechanism in unidirectional CFRP composites: Part I: Intralaminar toughness and AE characteristics. *Eng Fract Mech* 1999;64:721–45. doi:10.1016/S0013-7944(99)00096-X.
- [21] Rikards R. Interlaminar fracture behaviour of laminated composites. *Comput Struct* 2000;76:11–8. doi:10.1016/S0045-7949(99)00148-0.
- [22] Haj-Ali R, Kilic H. Nonlinear constitutive models for pultruded FRP composites. *Mech Mater* 2003;35:791–801. doi:10.1016/S0167-6636(02)00207-7.
- [23] Liu W, Feng P, Huang J. Bilinear softening model and double K fracture criterion for quasi-brittle fracture of pultruded FRP composites. *Compos Struct* 2017;160:1119–25. doi:10.1016/j.compstruct.2016.10.134.
- [24] Hutchinson JW, Suo Z. Mixed Mode Cracking in Layered Materials, 1991, p. 63–191. doi:10.1016/S0065-2156(08)70164-9.
- [25] Karihaloo BL. Fracture mechanics & structural concrete. Longman Sci Tech 1995.
- [26] Achintha M, Burgoyne C. fracture energy of the concrete–FRP interface in strengthened beams. *Eng Fract Mech* 2013;110:38–51. doi:10.1016/j.engfracmech.2013.07.016.
- [27] Oehlers DJ, Mohamed Ali MS, Haskett M, Lucas W, Muhamad R, Visintin P. FRP-Reinforced Concrete Beams: Unified Approach Based on IC Theory. *J Compos Constr* 2011;15:293–303. doi:10.1061/(ASCE)CC.1943-5614.0000173.
- [28] ASTM C29, Standard Test Method for Bulk Density and Voids in Aggregate, ASTM Inter., West Conshohocken, PA, USA, 2009 n.d.
- [29] Ross CA, Jerome DM, Tedesco JW, Hughes ML. Strengthening of reinforced concrete beams with externally bonded composite laminates. *Struct J* 1999;96:212–20.
- [30] Quantrill RJ, Hollaway LC, Thorne AM. Experimental and analytical investigation of FRP strengthened beam response: Part I. *Mag Concr Res* 1996;48:331–42. doi:10.1680/macr.1996.48.177.331.

- [31] R.Jones, R.N.Swamy, A.Charif. Plate separation and anchorage of RC beams strengthened by epoxy-bonded steel plates. *Struct Eng* 1988;66:85–94.
- [32] Garden HN, Quantrill RJ, Hollaway LC, Thorne AM, Parke GAR. An experimental study of the anchorage length of carbon fibre composite plates used to strengthen reinforced concrete beams. *Constr Build Mater* 1998;12:203–19. doi:10.1016/S0950-0618(98)00002-6.
- [33] Fanning PJ, Kelly O. Ultimate Response of RC Beams Strengthened with CFRP Plates. *J Compos Constr* 2001;5:122–7. doi:10.1061/(ASCE)1090-0268(2001)5:2(122).
- [34] Nguyen DM, Chan TK, Cheong HK. Brittle Failure and Bond Development Length of CFRP-Concrete Beams. *J Compos Constr* 2001;5:12–7. doi:10.1061/(ASCE)1090-0268(2001)5:1(12).
- [35] Gustafsson PJ, Hillerborg A. Improvements in Concrete Design Achieved Through the Application of Fracture Mechanics. *Appl. Fract. Mech. to Cem. Compos.*, Dordrecht: Springer Netherlands; 1985, p. 667–80. doi:10.1007/978-94-009-5121-1_24.
- [36] Guinea G V., Planas J, Elices M. A general bilinear fit for the softening curve of concrete. *Mater Struct* 1994;27:99–105. doi:10.1007/BF02472827.
- [37] Reinhardt HW. Crack softening zone in plain concrete under static loading. *Cem Concr Res* 1985;15:42–52. doi:10.1016/0008-8846(85)90007-9.
- [38] Bažant ZP, Becq-Giraudon E. Statistical prediction of fracture parameters of concrete and implications for choice of testing standard. *Cem Concr Res* 2002;32:529–56. doi:10.1016/S0008-8846(01)00723-2.
- [39] Roylance D. *Introduction to fracture mechanics* 2001.
- [40] Bazant ZP. *Fracture mechanics of concrete structures*. Proc First Int Conf Fract Mech Concr Struct Held Beaver Run Resort, Breckenridge, Colorado, USA 1992.
- [41] Emami MR, Abbaszadeh H. A comparison between intact and damaged compressive concrete specimens retrofitted by CFRP composites. 4th Natl Conf Civ Eng Archit Urban Manag Tehran, Iran 2017.